

# Summary

- Subject ID: ift20gazdev0700070
- Structural images: 1 T1-weighted (+ 2 T2-weighted)
- Functional series: 2
  - Task: TOM (1 run)
  - Task: resting (1 run)
- Standard output spaces: MNI152NLin2009cAsym
- Non-standard output spaces: T1w, func, run
- FreeSurfer reconstruction: Not run

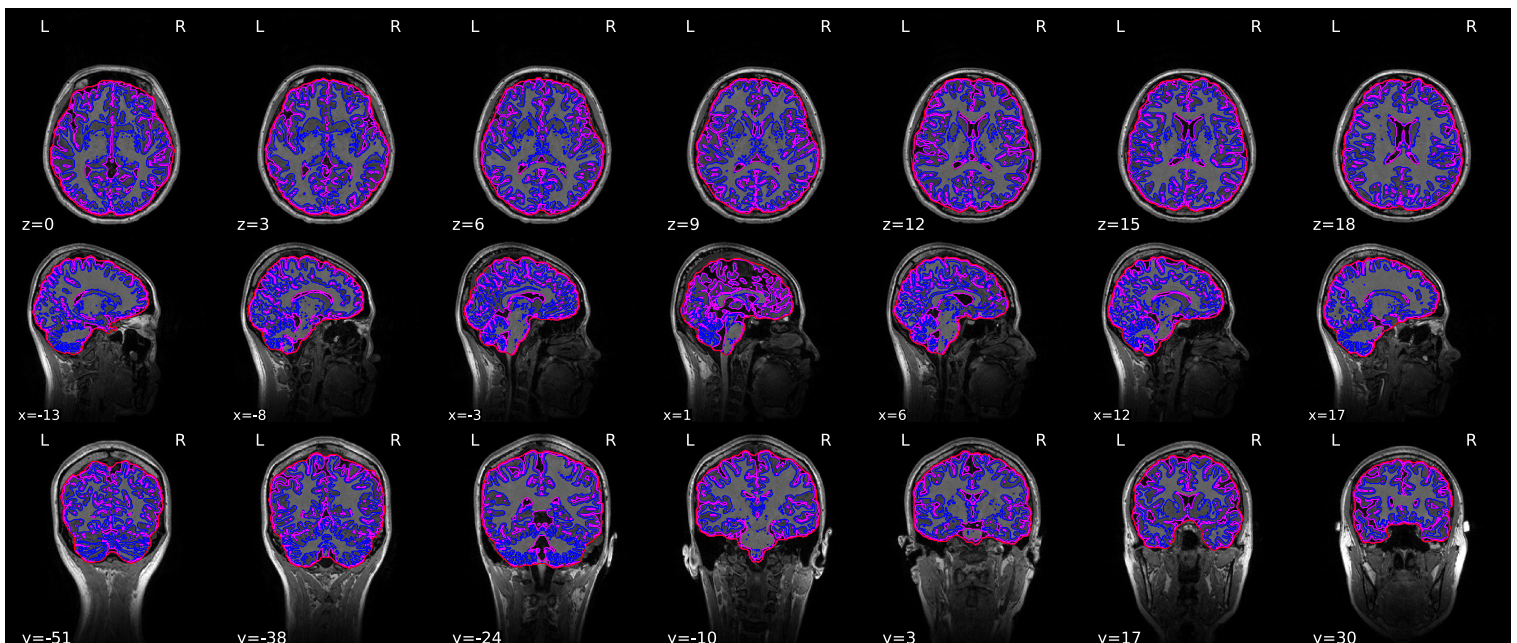
# Anatomical

## Anatomical Conformation

- Input T1w images: 1
- Output orientation: RAS
- Output dimensions: 208x256x256
- Output voxel size: 1mm x 1mm x 1mm
- Discarded images: 0

## Brain mask and brain tissue segmentation of the T1w

This panel shows the template T1-weighted image (if several T1w images were found), with contours delineating the detected brain mask and brain tissue segmentations.

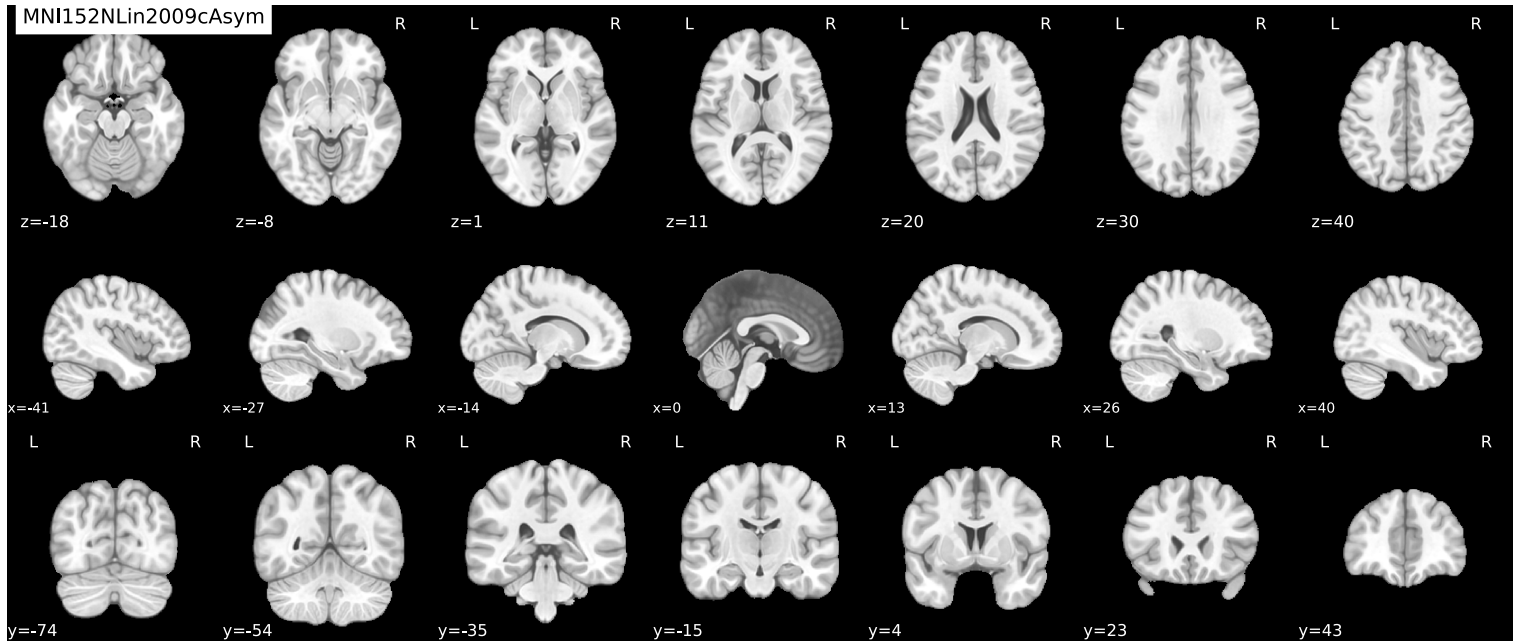


Get figure file: [sub-ift20gazdev0700070/figures/sub-ift20gazdev0700070\\_dseq.svg](sub-ift20gazdev0700070/figures/sub-ift20gazdev0700070_dseq.svg)

## Spatial normalization of the anatomical T1w reference

Results of nonlinear alignment of the T1w reference one or more template space(s). Hover on the panels with the mouse pointer to transition between both spaces.

Spatial normalization of the T1w image to the [MNI152NLin2009cAsym](#) template.



Get figure file: [sub-ift20gazdev0700070/figures/sub-ift20gazdev0700070\\_space-MNI152NLin2009cAsym\\_T1w.svg](sub-ift20gazdev0700070/figures/sub-ift20gazdev0700070_space-MNI152NLin2009cAsym_T1w.svg)

## Functional

### Reports for: task TOM, run 1.

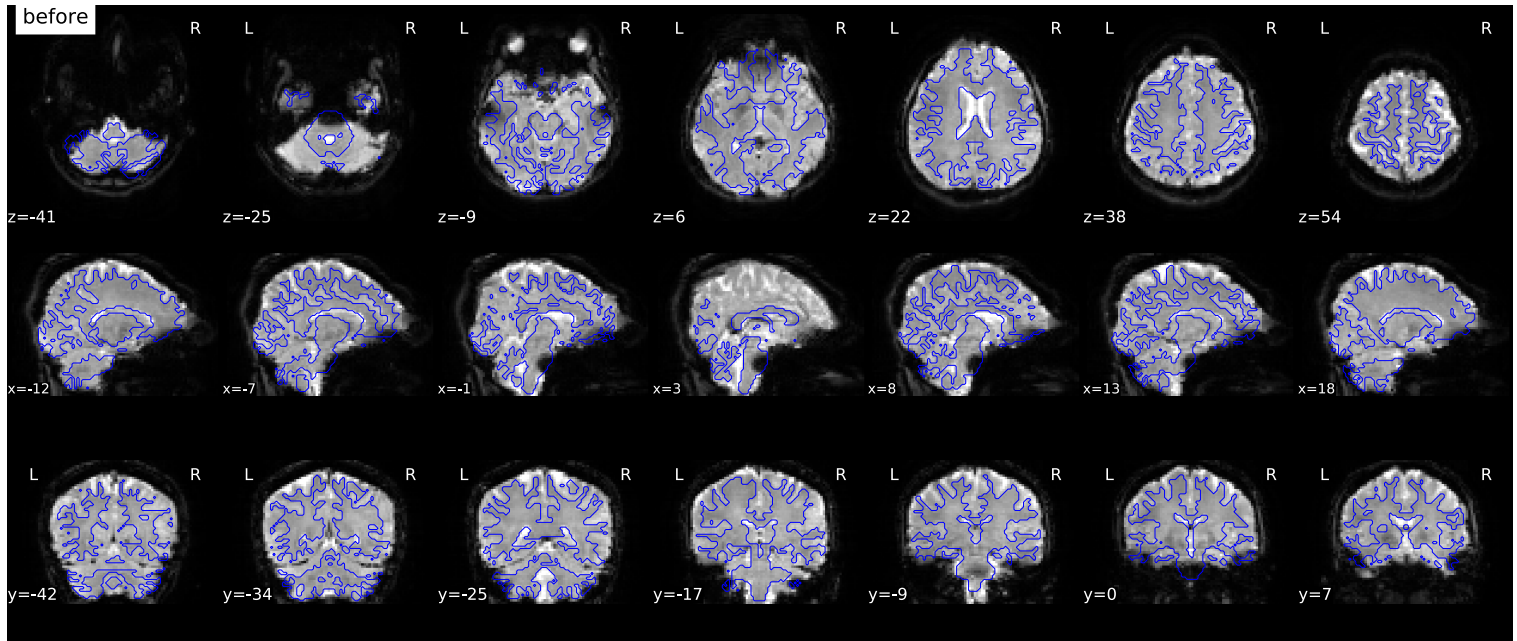
#### ▼ Summary

- Repetition time (TR): 0.8s
- Phase-encoding (PE) direction: Anterior-Posterior
- Single-echo EPI sequence.
- Slice timing correction: Not applied
- Susceptibility distortion correction: PEB/PEPOLAR (phase-encoding based / PE-POLARity)
- Registration: FSL `flirt` with boundary-based registration (BBR) metric - 6 dof
- Non-steady-state volumes: 7

#### ► Confounds collected

## Susceptibility distortion correction

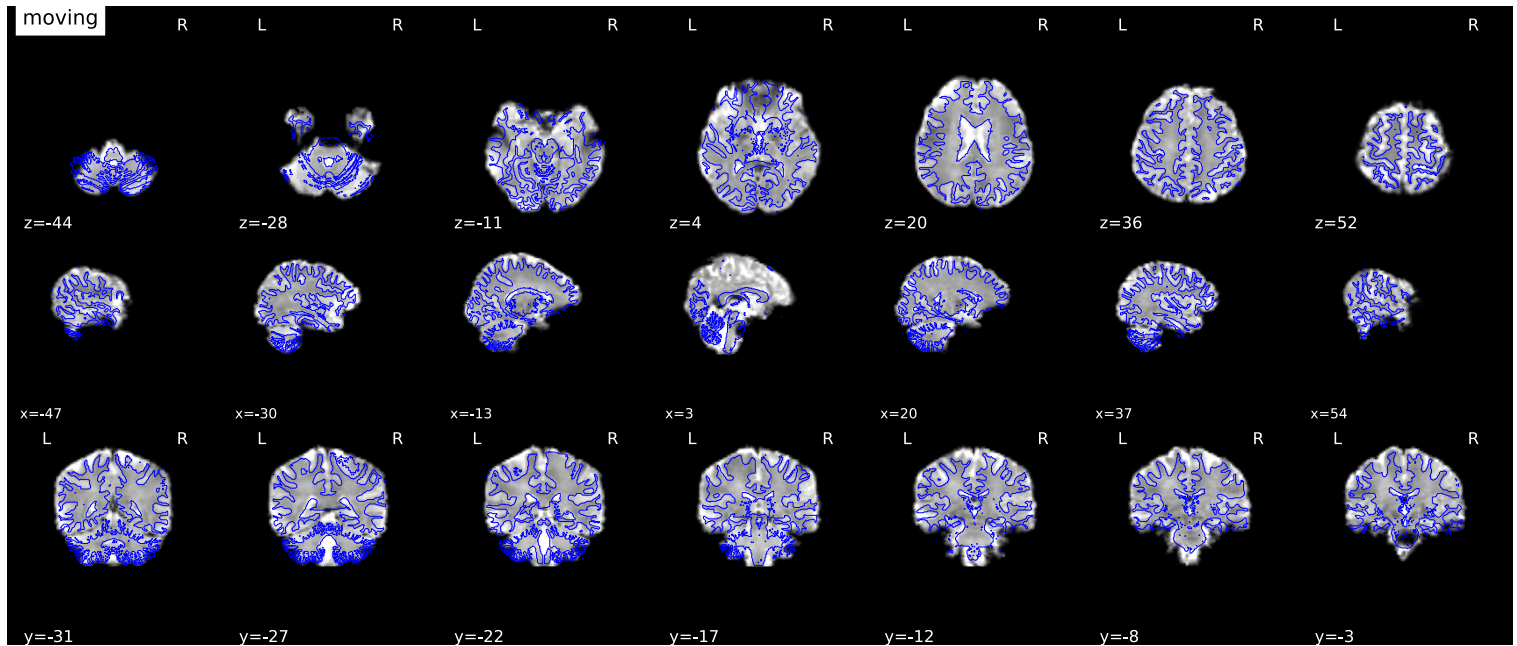
Results of performing susceptibility distortion correction (SDC) on the EPI



Get figure file: [sub-ift20gazdev0700070/figures/sub-ift20gazdev0700070 task-TOM\\_run-1\\_desc-sdc\\_bold.svg](https://openneuro.org/figures/sub-ift20gazdev0700070/task-TOM_run-1_desc-sdc_bold.svg)

## Alignment of functional and anatomical MRI data (surface driven)

FSL `flirt` was used to generate transformations from EPI-space to T1w-space - The white matter mask calculated with FSL `fast` (brain tissue segmentation) was used for BBR. Note that Nearest Neighbor interpolation is used in the reportlets in order to highlight potential spin-history and other artifacts, whereas final images are resampled using Lanczos interpolation.



Get figure file: [sub-ift20gazdev0700070/figures/sub-ift20gazdev0700070 task-TOM\\_run-1\\_desc-flirtbbr\\_bold.svg](https://openneuro.org/figures/sub-ift20gazdev0700070/task-TOM_run-1_desc-flirtbbr_bold.svg)

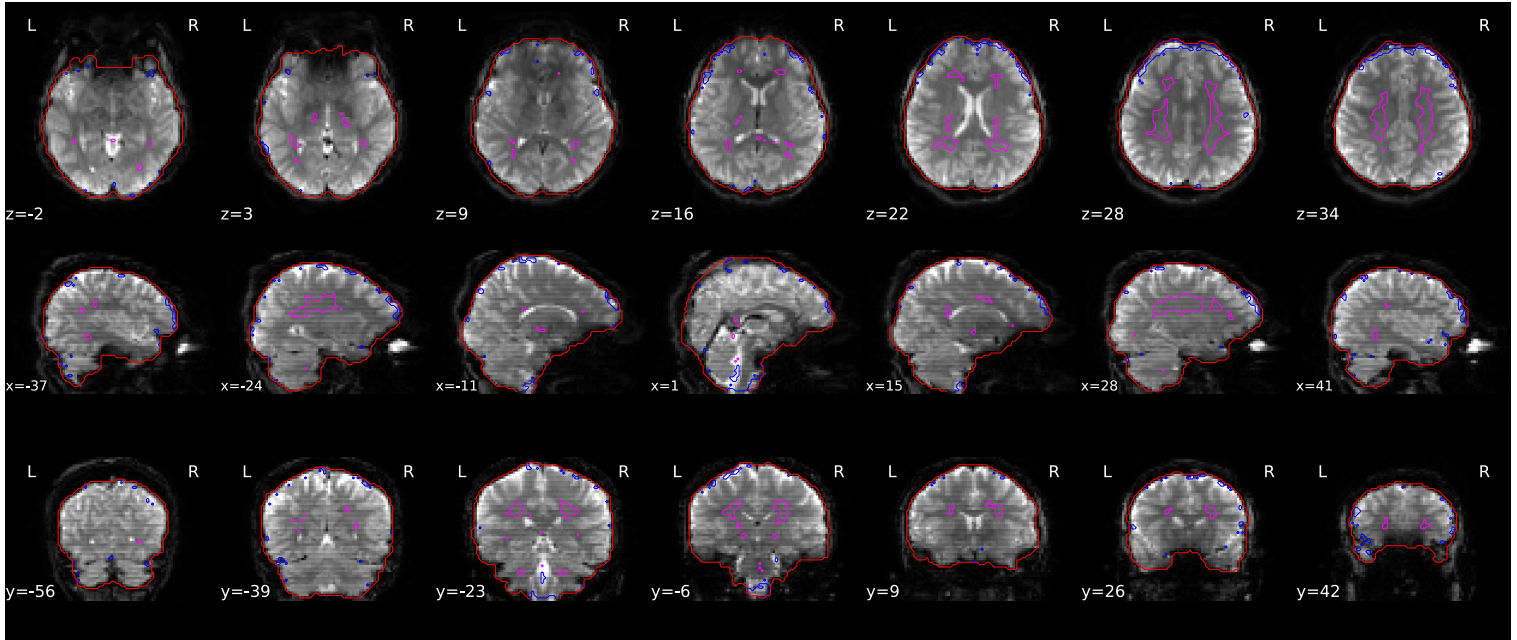
## Brain mask and (anatomical/temporal) CompCor ROIs

Brain mask calculated on the BOLD signal (red contour), along with the regions of interest (ROIs) used in *a/tCompCor* for extracting physiological and movement confounding components.

The *anatomical CompCor* ROI (magenta contour) is a mask combining CSF and WM (white-matter), where voxels containing a minimal

partial volume of GM have been removed.

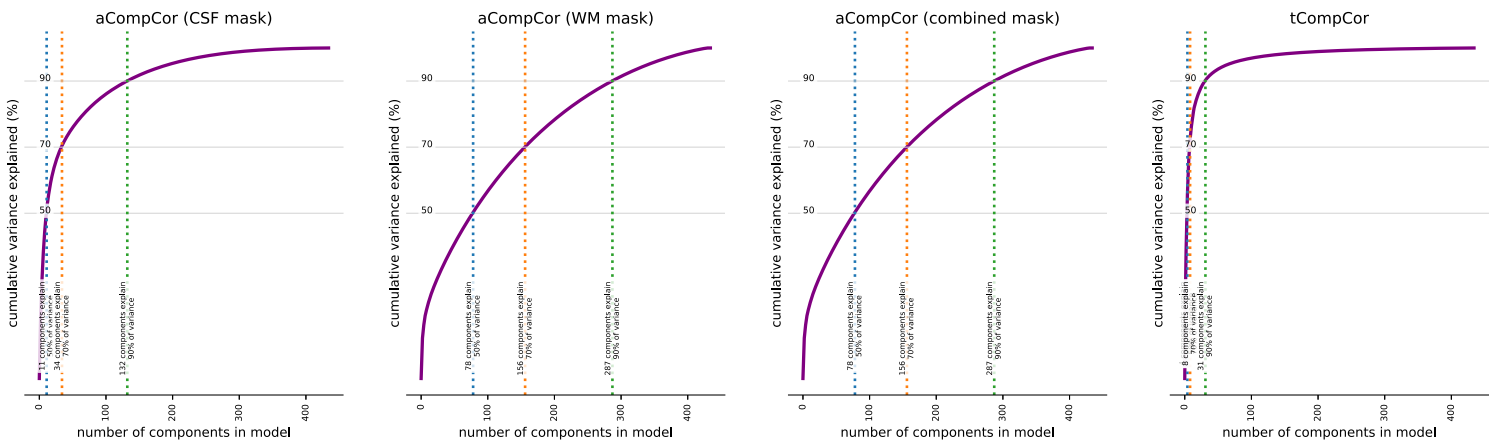
The *temporal CompCor* ROI (blue contour) contains the top 2% most variable voxels within the brain mask.



Get figure file: [sub-ift20gazdev0700070/figures/sub-ift20gazdev0700070 task-TOM run-1 desc-rois bold.svg](#)

## Variance explained by t/aCompCor components

The cumulative variance explained by the first  $k$  components of the *t/aCompCor* decomposition, plotted for all values of  $k$ . The number of components that must be included in the model in order to explain some fraction of variance in the decomposition mask can be used as a feature selection criterion for confound regression.



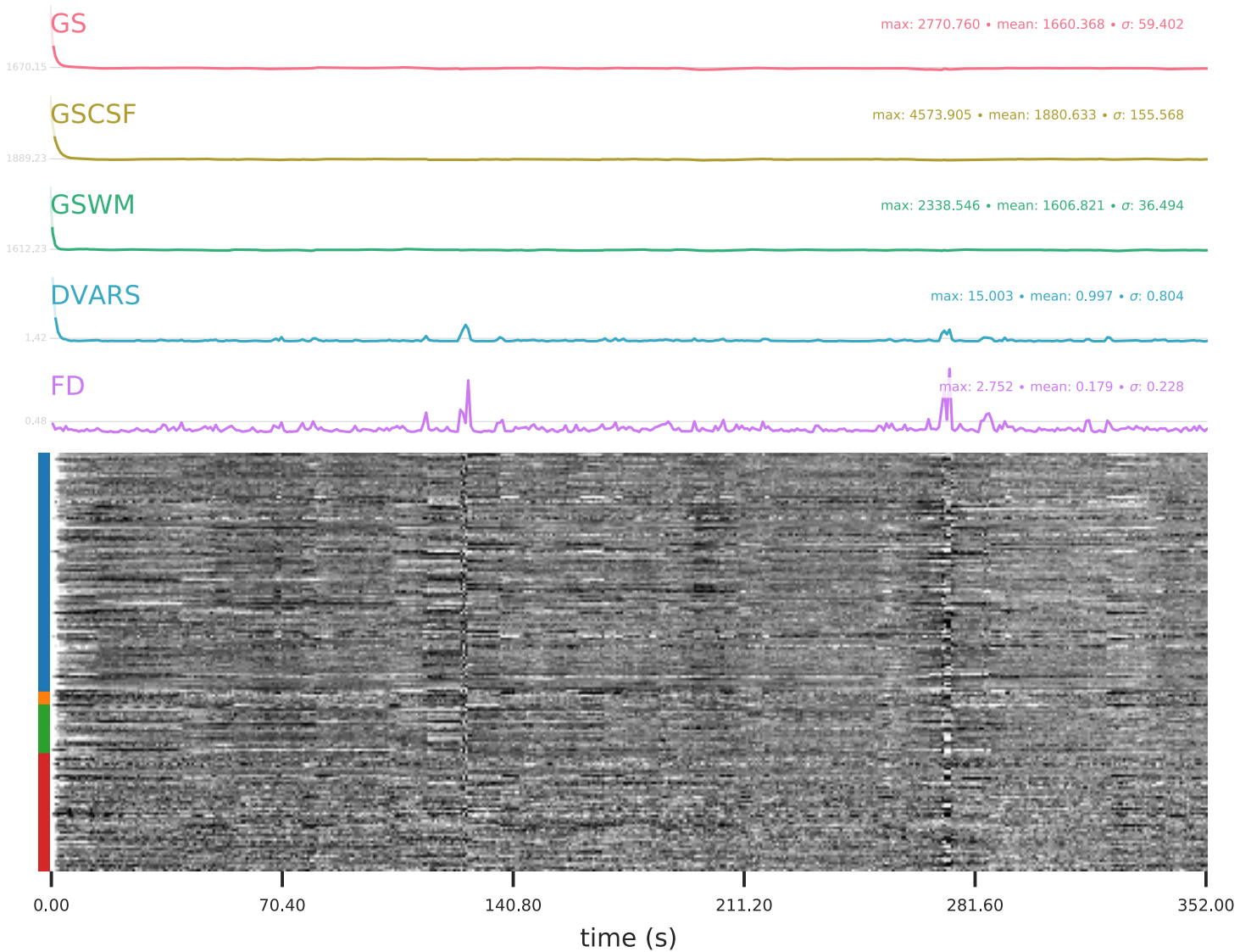
Get figure file: [sub-ift20gazdev0700070/figures/sub-ift20gazdev0700070 task-TOM run-1 desc-compcorvar bold.svg](#)

## BOLD Summary

Summary statistics are plotted, which may reveal trends or artifacts in the BOLD data. Global signals calculated within the whole-brain (GS), within the white-matter (WM) and within cerebro-spinal fluid (CSF) show the mean BOLD signal in their corresponding masks. DVARS and FD show the standardized DVARS and framewise-displacement measures for each time point.

A carpet plot shows the time series for all voxels within the brain mask, or if `--cifti-output` was enabled, all grayordinates. Voxels are grouped into cortical (dark/light blue), and subcortical (orange) gray matter, cerebellum (green) and white matter and CSF (red), indicated by the color map on the left-hand side.

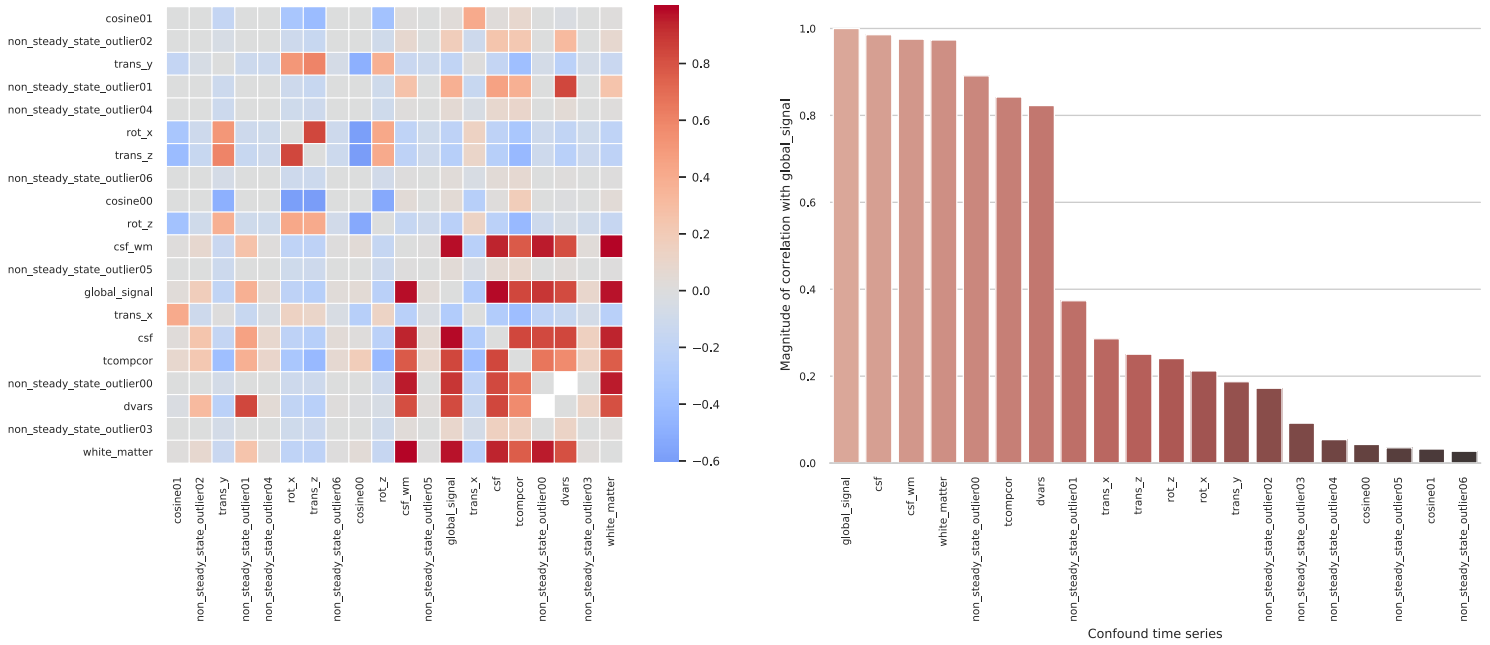




Get figure file: [sub-ift20gazdev0700070/figures/sub-ift20gazdev0700070\\_task-TOM\\_run-1\\_desc-carpetplot\\_bold.svg](https://openneuro.org/files/sub-ift20gazdev0700070/figures/sub-ift20gazdev0700070_task-TOM_run-1_desc-carpetplot_bold.svg)

## Correlations among nuisance regressors

Left: Heatmap summarizing the correlation structure among confound variables. (Cosine bases and PCA-derived CompCor components are inherently orthogonal.) Right: magnitude of the correlation between each confound time series and the mean global signal. Strong correlations might be indicative of partial volume effects and can inform decisions about feature orthogonalization prior to confound regression.



Get figure file: [sub-ift20gazdev0700070/figures/sub-ift20gazdev0700070\\_task-TOM\\_run-1\\_desc-confoundcorr\\_bold.svg](https://sub-ift20gazdev0700070/figures/sub-ift20gazdev0700070_task-TOM_run-1_desc-confoundcorr_bold.svg)

## Reports for: task resting.

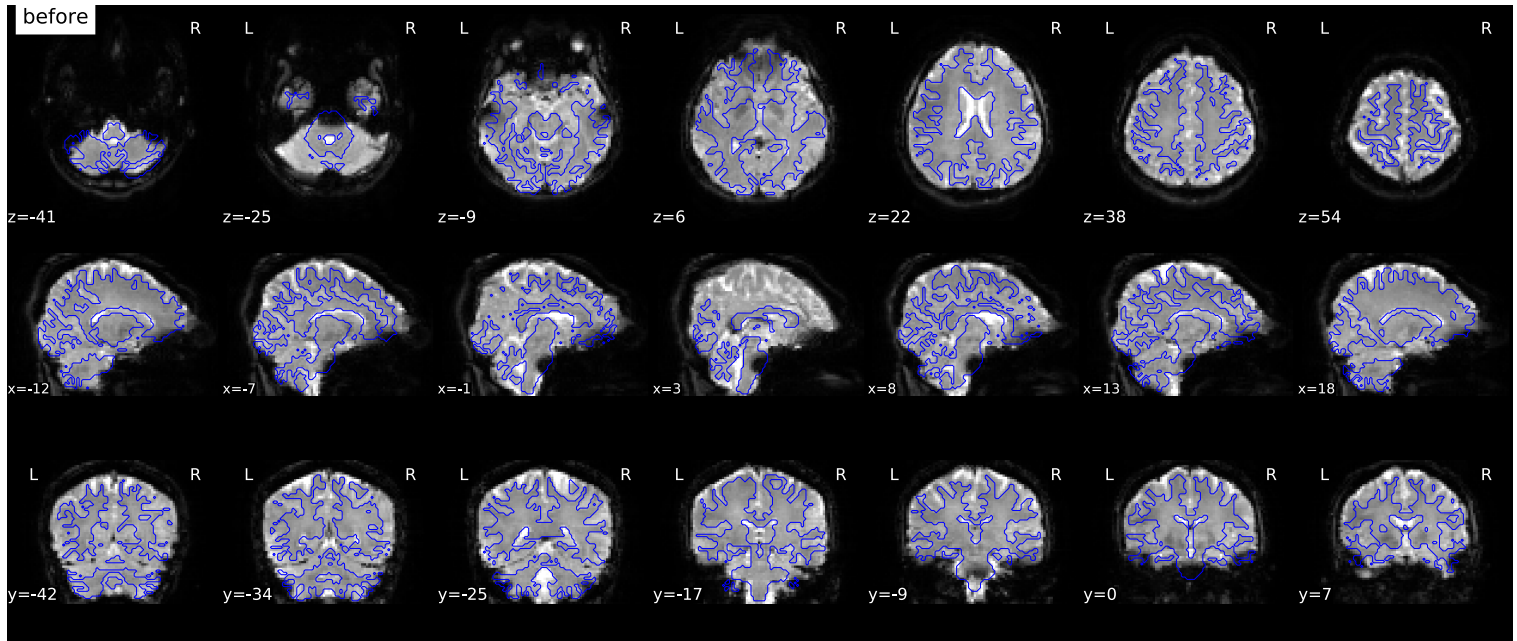
### ▼ Summary

- Repetition time (TR): 0.8s
- Phase-encoding (PE) direction: Anterior-Posterior
- Single-echo EPI sequence.
- Slice timing correction: Not applied
- Susceptibility distortion correction: PEB/PEPOLAR (phase-encoding based / PE-POLARity)
- Registration: FSL `flirt` with boundary-based registration (BBR) metric - 6 dof
- Non-steady-state volumes: 6

### ► Confounds collected

## Susceptibility distortion correction

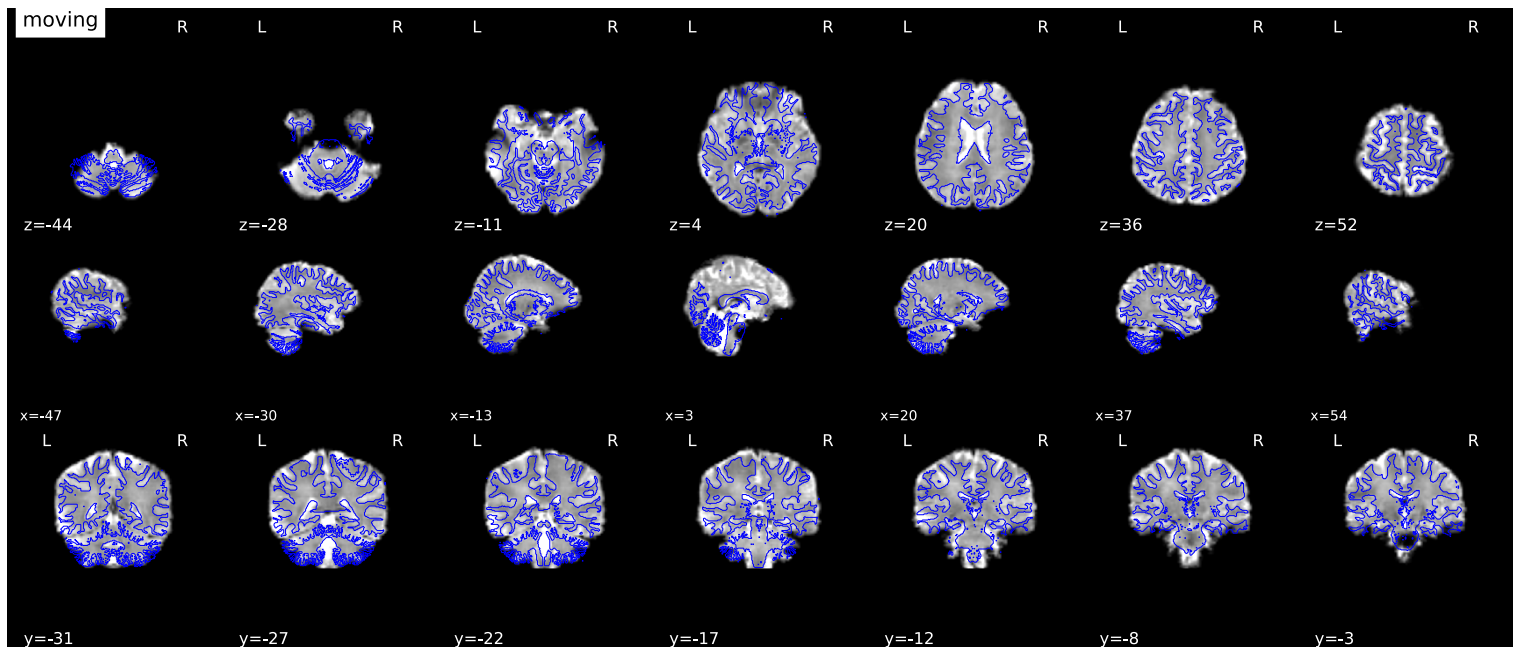
Results of performing susceptibility distortion correction (SDC) on the EPI



Get figure file: [sub-ift20gazdev0700070/figures/sub-ift20gazdev0700070 task-resting\\_desc-sdc\\_bold.svg](#)

## Alignment of functional and anatomical MRI data (surface driven)

FSL `flirt` was used to generate transformations from EPI-space to T1w-space - The white matter mask calculated with FSL `fast` (brain tissue segmentation) was used for BBR. Note that Nearest Neighbor interpolation is used in the reportlets in order to highlight potential spin-history and other artifacts, whereas final images are resampled using Lanczos interpolation.



Get figure file: [sub-ift20gazdev0700070/figures/sub-ift20gazdev0700070 task-resting\\_desc-flirtbbr\\_bold.svg](#)

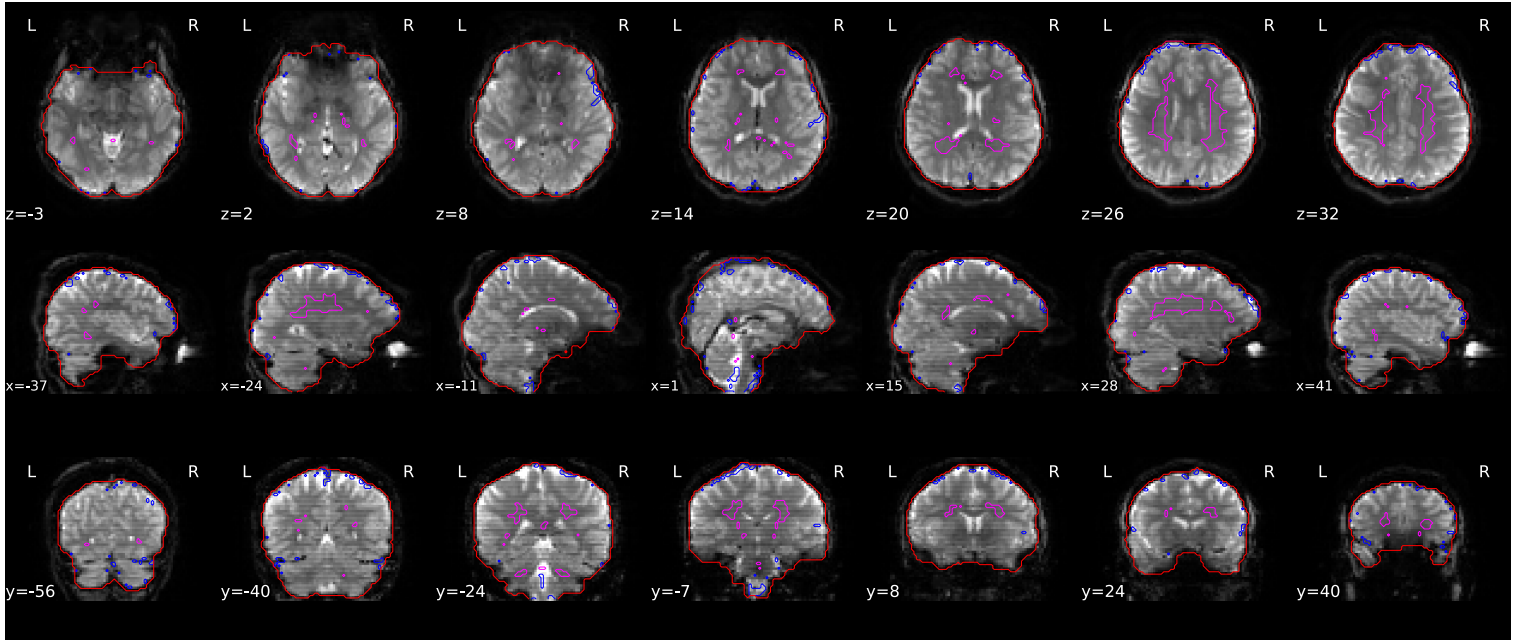
## Brain mask and (anatomical/temporal) CompCor ROIs

Brain mask calculated on the BOLD signal (red contour), along with the regions of interest (ROIs) used in *a/tCompCor* for extracting physiological and movement confounding components.

The *anatomical CompCor* ROI (magenta contour) is a mask combining CSF and WM (white-matter), where voxels containing a minimal

partial volume of GM have been removed.

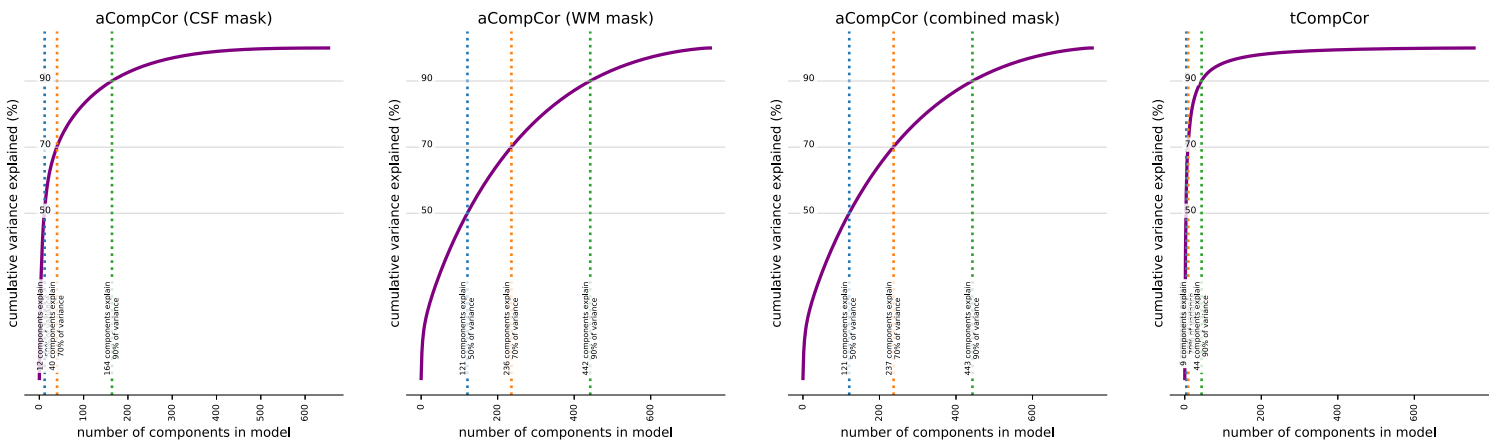
The *temporal CompCor* ROI (blue contour) contains the top 2% most variable voxels within the brain mask.



Get figure file: [sub-ift20gazdev0700070/figures/sub-ift20gazdev0700070 task-resting\\_desc-rois\\_bold.svg](#)

## Variance explained by t/aCompCor components

The cumulative variance explained by the first  $k$  components of the *t/aCompCor* decomposition, plotted for all values of  $k$ . The number of components that must be included in the model in order to explain some fraction of variance in the decomposition mask can be used as a feature selection criterion for confound regression.



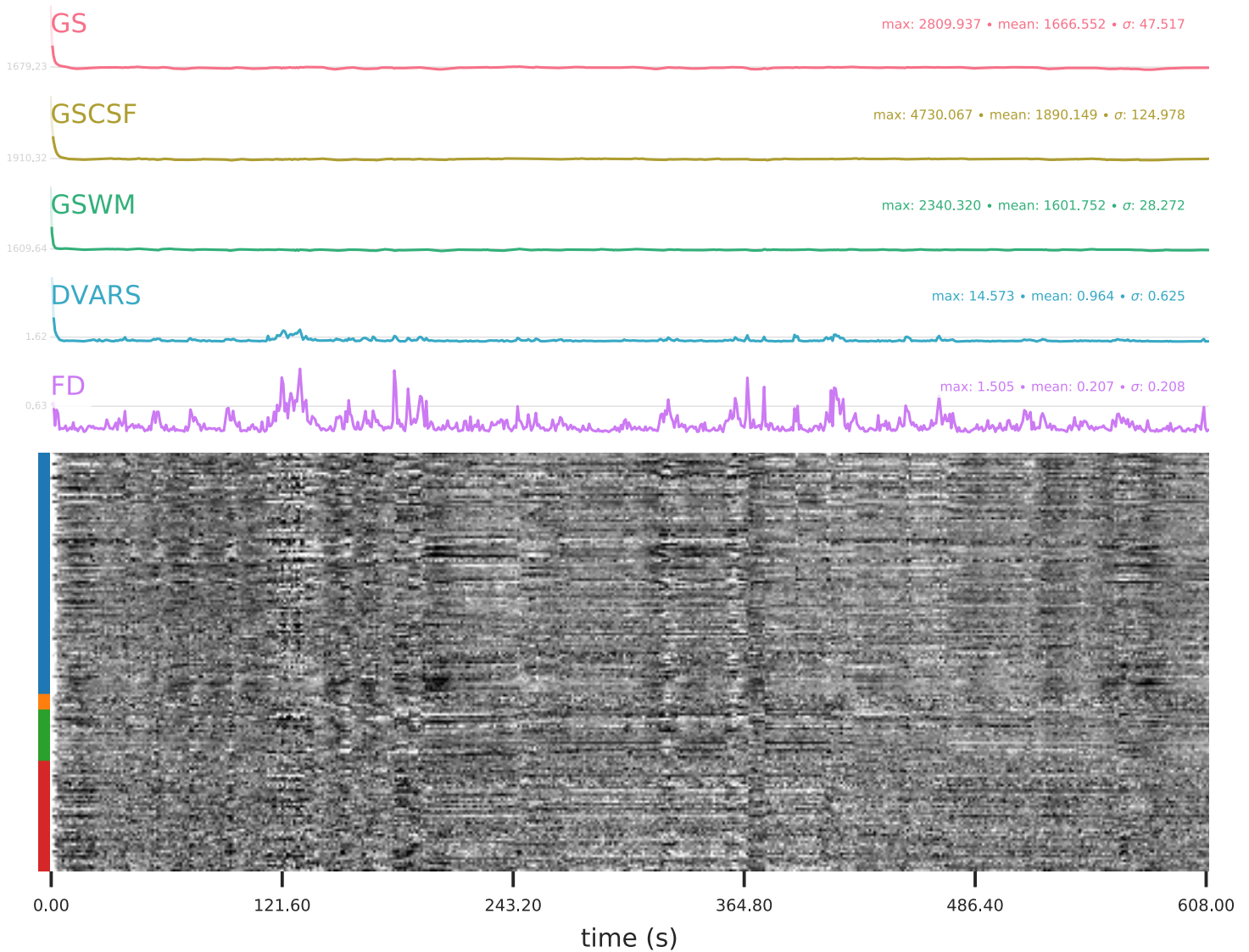
Get figure file: [sub-ift20gazdev0700070/figures/sub-ift20gazdev0700070 task-resting\\_desc-compcorvar\\_bold.svg](#)

## BOLD Summary

Summary statistics are plotted, which may reveal trends or artifacts in the BOLD data. Global signals calculated within the whole-brain (GS), within the white-matter (WM) and within cerebro-spinal fluid (CSF) show the mean BOLD signal in their corresponding masks. DVARS and FD show the standardized DVARS and framewise-displacement measures for each time point.

A carpet plot shows the time series for all voxels within the brain mask, or if `--cifti-output` was enabled, all grayordinates. Voxels are grouped into cortical (dark/light blue), and subcortical (orange) gray matter, cerebellum (green) and white matter and CSF (red), indicated by the color map on the left-hand side.

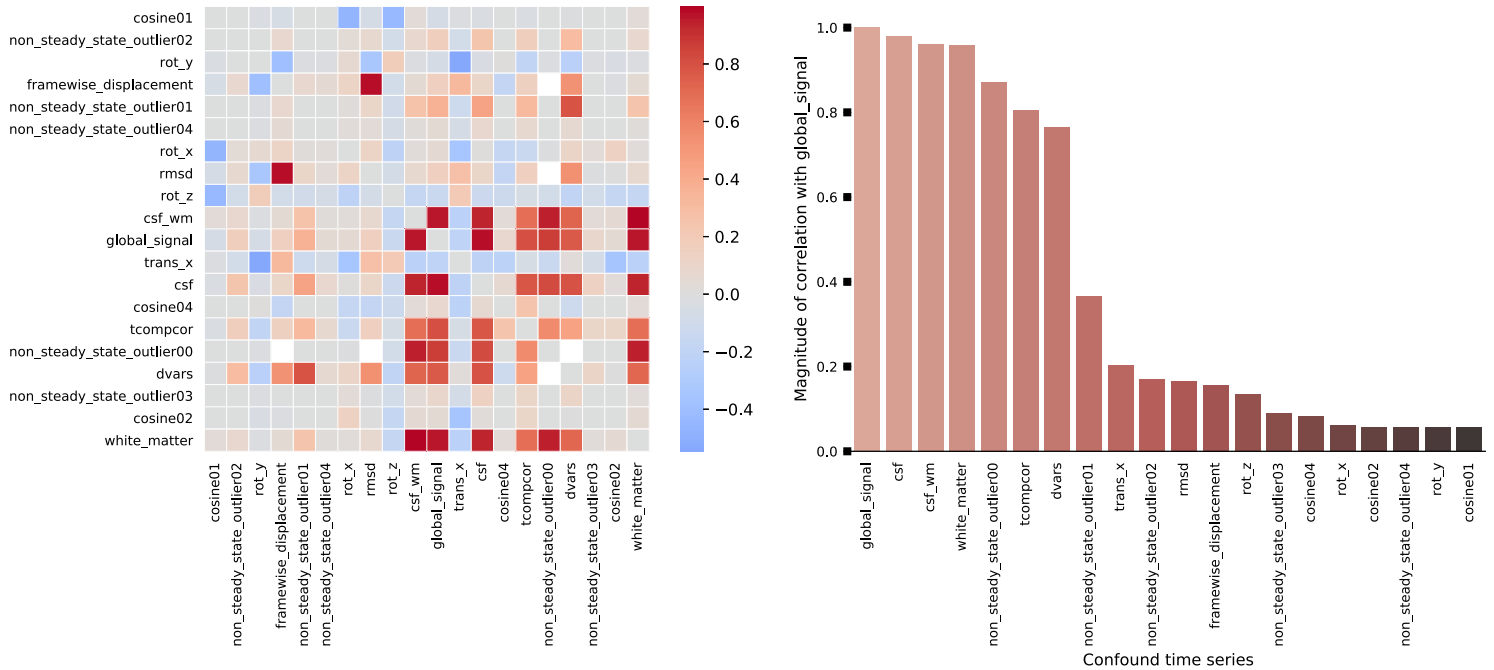




Get figure file: [sub-ift20gazdev0700070/figures/sub-ift20gazdev0700070 task-resting\\_desc-carpetplot\\_bold.svg](#)

## Correlations among nuisance regressors

Left: Heatmap summarizing the correlation structure among confound variables. (Cosine bases and PCA-derived CompCor components are inherently orthogonal.) Right: magnitude of the correlation between each confound time series and the mean global signal. Strong correlations might be indicative of partial volume effects and can inform decisions about feature orthogonalization prior to confound regression.



Get figure file: [sub-ift20gazdev0700070/figures/sub-ift20gazdev0700070\\_task-resting\\_desc-confoundcorr\\_bold.svg](https://sub-ift20gazdev0700070/figures/sub-ift20gazdev0700070_task-resting_desc-confoundcorr_bold.svg)

## About

- fMRIPrep version: 20.2.0
- fMRIPrep command: `/usr/local/miniconda/bin/fmriprep /home/klitinas/fmriprep/bids /home/klitinas/fmriprep/derivatives participant --participant-label=sub-ift20gazdev0700070 --nprocs 4 --fs-no-reconall -w /home/klitinas/fmriprep/work --skip_bids_validation --ignore_slicetiming sbref --output-spaces T1w func run MNI152NLin2009cAsym`
- Date preprocessed: 2021-08-10 08:55:35 -0400

## Methods

We kindly ask to report results preprocessed with this tool using the following boilerplate.

[HTML](#) [Markdown](#) [LaTeX](#)

Results included in this manuscript come from preprocessing performed using *fMRIPrep* 20.2.0 (Esteban, Markiewicz, et al. (2018); Esteban, Blair, et al. (2018); RRID:SCR\_016216), which is based on *Nipype* 1.5.1 (Gorgolewski et al. (2011); Gorgolewski et al. (2018); RRID:SCR\_002502).

### Anatomical data preprocessing

A total of 1 T1-weighted (T1w) images were found within the input BIDS dataset. The T1-weighted (T1w) image was corrected for intensity non-uniformity (INU) with *N4BiasFieldCorrection* (Tustison et al. 2010), distributed with ANTs 2.3.3 (Avants et al. 2008, RRID:SCR\_004757), and used as T1w-reference throughout the workflow. The T1w-reference was then skull-stripped with a *Nipype* implementation of the *antsBrainExtraction.sh* workflow (from ANTs), using OASIS3oANTs as target template. Brain tissue segmentation of cerebrospinal fluid (CSF), white-matter (WM) and gray-matter (GM) was performed on

the brain-extracted T1w using `fast` (FSL 5.0.9, RRID:SCR\_002823, Zhang, Brady, and Smith 2001). Volume-based spatial normalization to one standard space (MNI152NLin2009cAsym) was performed through nonlinear registration with `antsRegistration` (ANTs 2.3.3), using brain-extracted versions of both T1w reference and the T1w template. The following template was selected for spatial normalization: *ICBM 152 Nonlinear Asymmetrical template version 2009c* [Fonov et al. (2009), RRID:SCR\_008796; TemplateFlow ID: MNI152NLin2009cAsym],

### Functional data preprocessing

For each of the 2 BOLD runs found per subject (across all tasks and sessions), the following preprocessing was performed. First, a reference volume and its skull-stripped version were generated using a custom methodology of *fMRIPrep*. A B<sub>0</sub>-nonuniformity map (or *fieldmap*) was estimated based on two (or more) echo-planar imaging (EPI) references with opposing phase-encoding directions, with `3dQwarp` Cox and Hyde (1997) (AFNI 20160207). Based on the estimated susceptibility distortion, a corrected EPI (echo-planar imaging) reference was calculated for a more accurate co-registration with the anatomical reference. The BOLD reference was then co-registered to the T1w reference using `flirt` (FSL 5.0.9, Jenkinson and Smith 2001) with the boundary-based registration (Greve and Fischl 2009) cost-function. Co-registration was configured with nine degrees of freedom to account for distortions remaining in the BOLD reference. Head-motion parameters with respect to the BOLD reference (transformation matrices, and six corresponding rotation and translation parameters) are estimated before any spatiotemporal filtering using `mcflirt` (FSL 5.0.9, Jenkinson et al. 2002). The BOLD time-series (including slice-timing correction when applied) were resampled onto their original, native space by applying a single, composite transform to correct for head-motion and susceptibility distortions. These resampled BOLD time-series will be referred to as *preprocessed BOLD in original space*, or just *preprocessed BOLD*. The BOLD time-series were resampled into standard space, generating a *preprocessed BOLD run in MNI152NLin2009cAsym space*. First, a reference volume and its skull-stripped version were generated using a custom methodology of *fMRIPrep*. Several confounding time-series were calculated based on the *preprocessed BOLD*: framewise displacement (FD), DVARS and three region-wise global signals. FD was computed using two formulations following Power (absolute sum of relative motions, Power et al. (2014)) and Jenkinson (relative root mean square displacement between affines, Jenkinson et al. (2002)). FD and DVARS are calculated for each functional run, both using their implementations in *Nipype* (following the definitions by Power et al. 2014). The three global signals are extracted within the CSF, the WM, and the whole-brain masks. Additionally, a set of physiological regressors were extracted to allow for component-based noise correction (*CompCor*, Behzadi et al. 2007). Principal components are estimated after high-pass filtering the *preprocessed BOLD* time-series (using a discrete cosine filter with 128s cut-off) for the two *CompCor* variants: temporal (tCompCor) and anatomical (aCompCor). tCompCor components are then calculated from the top 2% variable voxels within the brain mask. For aCompCor, three probabilistic masks (CSF, WM and combined CSF+WM) are generated in anatomical space. The implementation differs from that of Behzadi et al. in that instead of eroding the masks by 2 pixels on BOLD space, the aCompCor masks are subtracted a mask of pixels that likely contain a volume fraction of GM. This mask is obtained by thresholding the corresponding partial volume map at 0.05, and it ensures components are not extracted from voxels containing a minimal fraction of GM. Finally, these masks are resampled into BOLD space and binarized by thresholding at 0.99 (as in the original implementation). Components are also calculated separately within the WM and CSF masks. For each *CompCor* decomposition, the *k* components with the largest singular values are retained, such that the retained components' time series are sufficient to explain 50 percent of variance across the nuisance mask (CSF, WM, combined, or temporal). The remaining components are dropped from consideration. The head-motion estimates calculated in the correction step were also placed within the corresponding confounds file. The confound time series derived from head motion estimates and global signals were expanded with the inclusion of temporal derivatives and quadratic terms for each (Satterthwaite et al. 2013). Frames that exceeded a threshold of 0.5 mm FD or 1.5 standardised DVARS were annotated as motion outliers. All resamplings can be performed with a *single interpolation step* by composing all the pertinent transformations (i.e. head-motion transform matrices, susceptibility distortion correction when available, and co-registrations to anatomical and output spaces). Gridded (volumetric) resamplings were performed using `antsApplyTransforms` (ANTs), configured with Lanczos interpolation to minimize the smoothing effects of other kernels (Lanczos 1964). Non-gridded (surface) resamplings were performed using `mri_vol2surf` (FreeSurfer).

Many internal operations of *fMRIPrep* use *Nilearn* 0.6.2 (Abraham et al. 2014, RRID:SCR\_001362), mostly within the functional processing workflow. For more details of the pipeline, see [the section corresponding to workflows in \*fMRIPrep\*'s documentation](#).

## Copyright Waiver

The above boilerplate text was automatically generated by *fMRIPrep* with the express intention that users should copy and paste this text into their manuscripts *unchanged*. It is released under the [CCo](#) license.

## References

- Abraham, Alexandre, Fabian Pedregosa, Michael Eickenberg, Philippe Gervais, Andreas Mueller, Jean Kossaifi, Alexandre Gramfort, Bertrand Thirion, and Gael Varoquaux. 2014. "Machine Learning for Neuroimaging with Scikit-Learn." *Frontiers in Neuroinformatics* 8. <https://doi.org/10.3389/fninf.2014.00014>.
- Avants, B.B., C.L. Epstein, M. Grossman, and J.C. Gee. 2008. "Symmetric Diffeomorphic Image Registration with Cross-Correlation: Evaluating Automated Labeling of Elderly and Neurodegenerative Brain." *Medical Image Analysis* 12 (1): 26–41. <https://doi.org/10.1016/j.media.2007.06.004>.
- Behzadi, Yashar, Khaled Restom, Joy Liau, and Thomas T. Liu. 2007. "A Component Based Noise Correction Method (CompCor) for BOLD and Perfusion Based fMRI." *NeuroImage* 37 (1): 90–101. <https://doi.org/10.1016/j.neuroimage.2007.04.042>.
- Cox, Robert W., and James S. Hyde. 1997. "Software Tools for Analysis and Visualization of fMRI Data." *NMR in Biomedicine* 10 (4-5): 171–78. [https://doi.org/10.1002/\(SICI\)1099-1492\(199706/08\)10:4/5<171::AID-NBM453>3.0.CO;2-L](https://doi.org/10.1002/(SICI)1099-1492(199706/08)10:4/5<171::AID-NBM453>3.0.CO;2-L).
- Esteban, Oscar, Ross Blair, Christopher J. Markiewicz, Shoshana L. Berleant, Craig Moodie, Feilong Ma, Ayse Ilkay Isik, et al. 2018. "fMRIPrep." *Software*. Zenodo. <https://doi.org/10.5281/zenodo.852659>.
- Esteban, Oscar, Christopher Markiewicz, Ross W Blair, Craig Moodie, Ayse Ilkay Isik, Asier Erramuzpe Aliaga, James Kent, et al. 2018. "fMRIPrep: A Robust Preprocessing Pipeline for Functional MRI." *Nature Methods*. <https://doi.org/10.1038/s41592-018-0235-4>.
- Fonov, VS, AC Evans, RC McKinstry, CR Alml, and DL Collins. 2009. "Unbiased Nonlinear Average Age-Appropriate Brain Templates from Birth to Adulthood." *NeuroImage* 47, Supplement 1: S102. [https://doi.org/10.1016/S1053-8119\(09\)70884-5](https://doi.org/10.1016/S1053-8119(09)70884-5).
- Gorgolewski, K., C. D. Burns, C. Madison, D. Clark, Y. O. Halchenko, M. L. Waskom, and S. Ghosh. 2011. "Nipype: A Flexible, Lightweight and Extensible Neuroimaging Data Processing Framework in Python." *Frontiers in Neuroinformatics* 5: 13. <https://doi.org/10.3389/fninf.2011.00013>.
- Gorgolewski, Krzysztof J., Oscar Esteban, Christopher J. Markiewicz, Erik Ziegler, David Gage Ellis, Michael Philipp Notter, Dorota Jarecka, et al. 2018. "Nipype." *Software*. Zenodo. <https://doi.org/10.5281/zenodo.596855>.
- Greve, Douglas N, and Bruce Fischl. 2009. "Accurate and Robust Brain Image Alignment Using Boundary-Based Registration." *NeuroImage* 48 (1): 63–72. <https://doi.org/10.1016/j.neuroimage.2009.06.060>.
- Jenkinson, Mark, Peter Bannister, Michael Brady, and Stephen Smith. 2002. "Improved Optimization for the Robust and Accurate Linear Registration and Motion Correction of Brain Images." *NeuroImage* 17 (2): 825–41. <https://doi.org/10.1006/nimg.2002.1132>.
- Jenkinson, Mark, and Stephen Smith. 2001. "A Global Optimisation Method for Robust Affine Registration of Brain Images." *Medical Image Analysis* 5 (2): 143–56. [https://doi.org/10.1016/S1361-8415\(01\)00036-6](https://doi.org/10.1016/S1361-8415(01)00036-6).



Lanczos, C. 1964. "Evaluation of Noisy Data." *Journal of the Society for Industrial and Applied Mathematics Series B Numerical Analysis* 1 (1): 76–85. <https://doi.org/10.1137/0701007>.

Power, Jonathan D., Anish Mitra, Timothy O. Laumann, Abraham Z. Snyder, Bradley L. Schlaggar, and Steven E. Petersen. 2014. "Methods to Detect, Characterize, and Remove Motion Artifact in Resting State fMRI." *NeuroImage* 84 (Supplement C): 320–41. <https://doi.org/10.1016/j.neuroimage.2013.08.048>.

Satterthwaite, Theodore D., Mark A. Elliott, Raphael T. Gerraty, Kosha Ruparel, James Loughhead, Monica E. Calkins, Simon B. Eickhoff, et al. 2013. "An improved framework for confound regression and filtering for control of motion artifact in the preprocessing of resting-state functional connectivity data." *NeuroImage* 64 (1): 240–56. <https://doi.org/10.1016/j.neuroimage.2012.08.052>.

Tustison, N. J., B. B. Avants, P. A. Cook, Y. Zheng, A. Egan, P. A. Yushkevich, and J. C. Gee. 2010. "N4ITK: Improved N<sub>3</sub> Bias Correction." *IEEE Transactions on Medical Imaging* 29 (6): 1310–20. <https://doi.org/10.1109/TMI.2010.2046908>.

Zhang, Y., M. Brady, and S. Smith. 2001. "Segmentation of Brain MR Images Through a Hidden Markov Random Field Model and the Expectation-Maximization Algorithm." *IEEE Transactions on Medical Imaging* 20 (1): 45–57. <https://doi.org/10.1109/42.906424>.

## Errors

No errors to report!